Journal of Chemistry and Technologies, 2025, *33*(4), 958-966

Journal of Chemistry and Technologies

pISSN 2663-2934 (Print), ISSN 2663-2942 (Online).

journal homepage: http://chemistry.dnu.dp.ua
editorial e-mail: chem.dnu@gmail.com

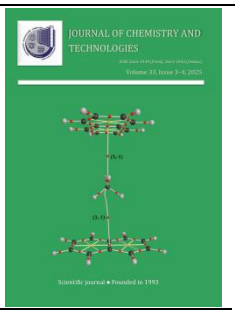

UDC 541.123.3

PHASE RELATION IN THE Fe_2O_3-Gd_2O_3 SYSTEM AT 1300 AND 1400 °C

Olga. V. Chudinovych[1,2], Anatoliy. V. Samelyuk[1], Serhiy. F. Korichev[1], Victor. S. Flis[3]

[1]*I. M. Frantsevich Institute for Problems in Materials Science NAS of Ukraine, 3, Omeliana Pritsaka St., 03142, Kyiv, Ukraine*
[2]*National Technical University of Ukraine «Igor Sikorsky Kyiv Polytechnic Institute», 37, Peremohy Ave., 03056, Kyiv, Ukraine*
[3]*G.V. Kurdyumov Institute for Metal Physics NAS of Ukraine, 36 Academician Vernadsky Blvd., 03142 Kyiv, Ukraine*

Received 4 August 2025; accepted 7 October 2025; available online 25 December 2025

Abstract

The phase interaction in the Fe_2O_3–Gd_2O_3 system at 1300 and 1400 °C were studied across the full concentration range using X-ray diffraction (XRD) and scanning electron microscopy (SEM). Samples, prepared in 1–5 mol% composition increments, were obtained by dissolving the oxides in HNO_3 (1 : 1), evaporating the solutions, and decomposing the nitrates at 800 °C for 2 h. The resulting powders were pressed at 10 MPa into 5 mm × 4 mm pellets and heat-treated in air at 1300 °C (300 h) and 1400 °C (100 h). The phase composition was determined using X-ray diffraction (XRD, DRON-3) and microstructural analysis (Superprobe-733, JEOL, Japan; Palo Alto, California, USA). At 1300 and 1400 °C, the isothermal sections of the Fe_2O_3–Gd_2O_3 phase diagram comprise four single-phase regions (B–Gd_2O_3, $GdFeO_3$(R), $Gd_3Fe_5O_{12}$, Fe_2O_3) and three two-phase regions (B–Gd_2O_3 + $GdFeO_3$, $GdFeO_3$ + $Gd_3Fe_5O_{12}$, $Gd_3Fe_5O_{12}$ + Fe_2O_3). The concentration dependence of the unit cell parameters for phases in the studied system was established. In the Fe_2O_3–Gd_2O_3 system at 1300 and 1400 °C, an ordered perovskite-type phase with orthorhombic distortion ($GdFeO_3$) is formed. Its homogeneity range at both temperatures extends from 48 to 52 mol.% Gd_2O_3.

Keywords: phase equilibria; iron oxide; gadolinium oxide; perovskite-type; solid solutions; lattice parameters.

ФАЗОВІ РІВНОВАГИ В СИСТЕМІ Fe_2O_3-Gd_2O_3 ЗА 1300 ТА 1400 °C

Ольга В. Чудінович[1,2], Анатолій В. Самелюк[1], Сергій Ф. Корічев[1], Віктор С. Фліс[3]

[1]*Інститут проблем матеріалознавства ім. І.М. Францевича НАН України, вул. Омеляна Пріцака, 3, Київ, Україна, 03142*
[2]*Національний технічний університет України "Київський політехнічний інститут імені Ігоря Сікорського", просп. Перемоги, 37, м. Київ, Україна, 03056*
[3]*Інститут металофізики імені Г.В. Курдюмова НАН України, бульвар академіка Вернадського, 36, 03142 Київ, Україна*

Анотація

Досліджені фазові співвідношення в системі Fe_2O_3–Gd_2O_3 за 1300 та 1400 °C в усьому концентраційному інтервалі за допомогою рентгенівської дифракції (XRD) та скануючої електронної мікроскопії (SEM). Концентраційний крок становив 1–5 мол.%. Гадоліній (III) оксид розчиняли в HNO_3 (1 : 1) з подальшим випаровуванням розчинів та розкладанням нітратів за 800 °C протягом 2 год. Порошки пресували під тиском 10 МПа в таблетки діаметром 5 мм та висотою 4 мм. Термообробку зразків проводили за 1300 °C (300 год) та 1400 °C (100 год) у повітрі. Дослідження фазового складу проводили з використанням рентгенівської дифракції (XRD, DRON-3) та мікроструктурного аналізу (Superprobe-733, JEOL, Японія, Пало-Альто, Каліфорнія). За температур 1300 та 1400 °C ізотермічні перерізи фазової діаграми Fe_2O_3–Gd_2O_3 складаються з чотирьох однофазних зон (B–Gd_2O_3, $GdFeO_3$(R), $Gd_3Fe_5O_{12}$, Fe_2O_3) та трьох двофазних зон (B–Gd_2O_3+$GdFeO_3$, $GdFeO_3$+$Gd_3Fe_5O_{12}$, $Gd_3Fe_5O_{12}$+Fe_2O_3). Побудовані залежності параметрів елементарної комірки фаз від концентрації у досліджуваній системі. Для системи Fe_2O_3–Gd_2O_3 за 1300 та 1400 °C характерне утворення впорядкованої перовськітної фази з ромбічним спотворенням ($GdFeO_3$). У системі Fe_2O_3–Gd_2O_3 за 1300 та 1400 °C утворюється впорядкована фаза типу перовскіту з ромбічним спотворенням ($GdFeO_3$). Її область гомогенності за обох температур становить від 48 до 52 мол.% Gd_2O_3.

Ключові слова: фазові рівноваги; феррум (III) оксид; гадоліній (III) оксид; перовскіт; тверді розчини; параметри елементарної комірки.

**Corresponding author: email: chudinovych_olia@ukr.net*

doi: 10.15421/jchemtech.v33i4.336812

Journal of Chemistry and Technologies, 2025, *33*(4), 958-966

Introduction

Oxides of transition and rare-earth elements remain the subject of intensive research due to their wide range of functional properties, which determine their suitability for use in electronics, spintronics, magnetic technologies, and biomedicine. In particular, iron oxide (Fe_2O_3) and gadolinium oxide (Gd_2O_3) are of interest both individually and as part of multicomponent systems, as they combine magnetic activity, thermal stability, chemical inertness, and the ability to form complex crystalline phases [1]. Fe_2O_3 is a well-known ferromagnetic material used in pigments, magnets, sensors, and storage devices. Gd_2O_3, in turn, is characterized by high paramagnetic susceptibility, as well as radiation and thermal stability, which makes it a promising component in laser technology, nuclear reactors, and as a contrast agent for magnetic resonance imaging (MRI) [2]. The combination of Fe_2O_3 and Gd_2O_3 in the form of composites, nanostructured materials, or solid solutions allows the creation of functional systems with enhanced properties, such as bimodal magnetic contrast (T_1/T_2), high resistance to aggressive environments, and stable operation over a wide temperature range [3–5]. Orthoferrites of rare earth elements with the general formula $LnFeO_3$ (where Ln = La–Lu) belong to the class of oxide perovskite phases with orthorhombic symmetry (space group Pbnm) [6–15]. Due to the combination of characteristic structural features and multifunctional physicochemical properties, these compounds are widely used in spintronics, magneto-optics, photocatalysis, sensor systems, and biomedical technologies [6–15]. Hybrid Fe_2O_3–Gd_2O_3 nanoparticles have already been successfully employed as theranostic agents, combining tumor imaging with targeted drug delivery [16–17]. Moreover, these materials demonstrate promising potential in adaptive magnetorheological fluids, magnetic refrigeration, sensing technologies, and high-frequency electronics [18–19].

The phase interaction between Fe_2O_3 and Gd_2O_3 is of particular significance. According to Musić and co-workers [20-21], the system forms α-Fe_2O_3, $GdFeO_3$, $Gd_3Fe_5O_{12}$, and Gd_2O_3 phases depending on temperature and stoichiometry. Gamma-ray resonance (Mössbauer) spectroscopy confirms the absence of solid solution formation, instead revealing the presence of well-defined crystalline phases. Diffusion studies in vapor at 1200–1400 °C show parabolic growth kinetics of $GdFeO_3$ (perovskite) and $Gd_3Fe_5O_{12}$ (garnet) layers, associated with limited diffusion of the corresponding ions: Gd^{3+} and O^{2-} for the garnet, Fe^{3+} and O^{2-} for the perovskite [22]. The obtained activation energy values (≈550 kJ mol^{-1} for $Gd_3Fe_5O_{12}$ and ≈400 kJ mol^{-1} for $GdFeO_3$) indicate the complexity of phase formation processes in this system.

Modern research also explores mechanochemical, thermochemical, and electrochemical methods for synthesizing such materials. In particular, electrolysis of an oxide mixture in molten $CaCl_2$ (the FFC Cambridge process) enables the formation of intermetallic phases Gd_2Fe_{17} and $GdFe_2$ at 900 °C [23], offering promising prospects for producing next-generation magnetic materials directly from oxide precursors.

Therefore, the investigation of thermodynamics, phase equilibria, and compound morphology in the Gd_2O_3–Fe_2O_3 system is relevant from both scientific and practical perspectives. This study aims to examine phase interactions in the iron oxide–gadolinium oxide system and to determine the homogeneity limits of the resulting phases.

Materials and Methods

Gd_2O_3 with a main component content of 99.99 %, $Fe(NO_3)_3 \cdot 9H_2O$, and nitric acid were employed as the starting materials. Samples with different iron oxide Fe_2O_3 contents (from 0 to 100 mol%) were obtained from nitrate solutions of gadolinium (Gd^{3+}) and iron (Fe^{3+}). After evaporation of the solutions, they were decomposed at 800 °C for 2 hours. Solutions of Gd^{3+} nitrates were obtained by dissolving gadolinium oxide in nitric acid. The resulting powders were pressed at 10 MPa into 5 mm × 4 mm pellets. To study phase relationships at 1300 and 1400 °C thermal treatment of as-prepared samples was carried out in two stages: at 1100 °C (for 100 h in air) and then at 1300 °C (for 300 h in air) and 1400 °C (for 100 h in air) in the furnaces with heating elements based on Fecral (H23U5T) and Superkanthal ($MoSi_2$), respectively. The heating rate was 3 °C/min^{-1}.

The phase composition was determined using X-ray diffraction (XRD, DRON-3) and microstructural analysis (Superprobe-733, JEOL, Japan; Palo Alto, California, USA).

For the analysis of the phase composition, a DRON-3M X-ray diffractometer (CuKα radiation, nickel filter) was used. The scanning speed of 0.05–0.1° 2θ/min was employed in the 15° to 90° 2θ range. Lattice parameters were refined by least squares fitting using the LATTIC program.

Journal of Chemistry and Technologies, 2025, *33*(4), 958-966

The effective precision of the measurements was ± 0.0002 nm. Phase composition has been determined with the aid of International powder standards (JSPDS International Center for Diffraction Data 1999). The homogeneity of the powders was evaluated by scanning electron microscopy (SEM). Elemental analysis of the samples was carried out by X-ray spectral microanalysis.

Results and discussion

The chemical and phase compositions in Fe_2O_3–Gd_2O_3 system annealed at 1300 and 1400 °C with lattice parameters are summarized in Table 1, Table 2 and Table 3, respectively. The results were used to plot the isothermal section of the Fe_2O_3–Gd_2O_3 phase diagram at 1300 and 1400 °C (Fig. 1).

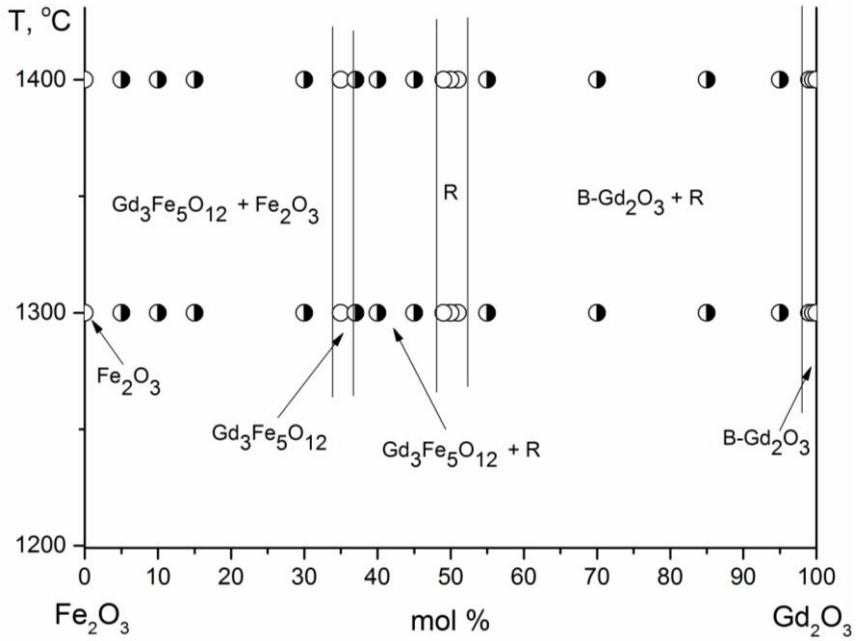

Fig. 1. Isothermal section at 1300 and 1400 °C for the system Fe_2O_3–Gd_2O_3 (○ – single-phase samples, ◐ - two-phase samples)

Table 1

Phase composition and lattice parameters of the phases in the Fe_2O_3–Gd_2O_3 system, annealed at 1300 °C for 300 h in air (XRD and SEM data)

Chemical composition, mol%		Phases by XRD	Lattice parameters of the phases σ ± 0.0002, nm								
Fe_2O_3	Gd_2O_3		R			Fe_2O_3		B-Gd_2O_3			
			a	*b*	*c*	*a*	*c*	*a*	*b*	*c*	*β*
100	0	Fe_2O_3				0.511	1.382				
95	5	Fe_2O_3 + $Gd_3Fe_5O_{12}$				0.504	1.375				
90	10	Fe_2O_3 + $Gd_3Fe_5O_{12}$				0.505	1.369				
85	15	Fe_2O_3 + $Gd_3Fe_5O_{12}$				0.503	1.377				
70	30	Fe_2O_3 + $Gd_3Fe_5O_{12}$									
65	35	$Gd_3Fe_5O_{12}$									
63	37	R + $Gd_3Fe_5O_{12}$									
60	40	R + $Gd_3Fe_5O_{12}$									
55	45	R + $Gd_3Fe_5O_{12}$	0.560	0.764	0.533						
51	49	R	0.559	0.766	0.533						
50	50	R	0.558	0.766	0.535						
49	51	R	0.559	0.766	0.534						
45	55	R +B-Gd_2O_3	0.560	0.782	0.532			1.410	0.326	0.947	78.92
30	70	R +B-Gd_2O_3	0.560	0.765	0.534			1.432	0.344	0.896	86.47
15	85	R +B-Gd_2O_3	0.559	0.767	0.532			1.429	0.351	0.978	89.89
5	95	R +B-Gd_2O_3						1.515	0.358	0.958	92.15
2	98	B-Gd_2O_3						1.442	0.357	0.879	84.86
1	99	B-Gd_2O_3						1.437	0.354	1.012	85.78
0.5	99,5	B-Gd_2O_3						1.441	0.354	0.938	86.74
0	100	B-Gd_2O_3						1.409	0.357	0.876	100.0

Journal of Chemistry and Technologies, 2025, *33*(4), 958-966

Table 2

Phase composition and lattice parameters of the phases in the Fe_2O_3–Gd_2O_3 system, annealed at 1300 and 1400°C in air (XRD and SEM data)

Chemical composition, mol%		Phases by XRD	Lattice parameters of the $Gd_3Fe_5O_{12}$ phase σ ± 0.0002, nm	
Fe_2O_3	Gd_2O_3		1300	1400
			a	*a*
95	5	Fe_2O_3 + $Gd_3Fe_5O_{12}$	1.249	1.243
90	10	Fe_2O_3 + $Gd_3Fe_5O_{12}$	1.250	1.244
85	15	Fe_2O_3 + $Gd_3Fe_5O_{12}$	1.249	1.245
70	30	Fe_2O_3 + $Gd_3Fe_5O_{12}$	1.247	1.246
65	35	$Gd_3Fe_5O_{12}$	1.246	1.246
63	37	R + $Gd_3Fe_5O_{12}$	1.245	1.245
60	40	R + $Gd_3Fe_5O_{12}$	1.245	1.245
55	45	R + $Gd_3Fe_5O_{12}$	1.248	1.240

Table 3

Phase composition and lattice parameters of the phases in the Fe_2O_3–Gd_2O_3 system, annealed at 1400 °C for 100 h in air (XRD and SEM data)

Chemical composition, mol%		Phases by XRD	Lattice parameters of the phases σ ± 0.0002, nm								
Fe_2O_3	Gd_2O_3		R			Fe_2O_3		B-Gd_2O_3			
			a	*b*	*c*	*a*	*c*	*a*	*b*	*c*	*β*
100	0	Fe_2O_3				0.511	1.382				
95	5	Fe_2O_3 + $Gd_3Fe_5O_{12}$				0.503	1.374				
90	10	Fe_2O_3 + $Gd_3Fe_5O_{12}$				0.503	1.369				
85	15	Fe_2O_3 + $Gd_3Fe_5O_{12}$				0.503	1.371				
70	30	Fe_2O_3 + $Gd_3Fe_5O_{12}$									
65	35	$Gd_3Fe_5O_{12}$									
63	37	R + $Gd_3Fe_5O_{12}$									
60	40	R + $Gd_3Fe_5O_{12}$									
55	45	R + $Gd_3Fe_5O_{12}$	0.560	0.764	0.533						
51	49	R	0.559	0.766	0.533						
50	50	R	0.558	0.766	0.535						
49	51	R	0.559	0.766	0.534						
45	55	R + B-Gd_2O_3	0.560	0.782	0.532						
30	70	R + B-Gd_2O_3	0.560	0.765	0.534			1.437	0.358	0.858	86.80
15	85	R + B-Gd_2O_3	0.559	0.767	0.532			1.434	0.370	0.872	90.28
5	95	R + B-Gd_2O_3						1.434	0.354	0.882	91.25
2	98	B-Gd_2O_3						1.435	0.355	0.870	91.56
1	99	B-Gd_2O_3						1.436	0.357	0.859	91.57
0.5	99,5	B-Gd_2O_3						1.405	0.320	0.873	79.75
0	100	B-Gd_2O_3						1.409	0.357	0.876	100.0

According to SEM and XRD analyses, Figs. 2, 3, 4 respectively, there are Gd_2O_3, Fe_2O_3, $Gd_3Fe_5O_{12}$ and $GdFeO_3$ (R) phases in the Fe_2O_3–Gd_2O_3 system at 1300 and 1400 °C.

In the system Fe_2O_3–Gd_2O_3 at 1300 and 1400 °C, an ordered phase of perovskite-type with orthorhombic distortion has been revealed. It was found that at 1300 °C and 1400 °C, the homogeneity region of the $GdFeO_3$ (R) phase is in the range from 48 to 52 mol% Gd_2O_3, Fig. 5a, b, c. The lattice parameters of the unit cell R phase varies from a = 0.563 nm, b = 0.764 nm, c = 0.533 nm in two-phase sample ($Gd_3Fe_5O_{12}$ + R), containing 40 mol % Gd_2O_3-60 mol % Fe_2O_3 to a = 0.561 nm, b = 0.768 nm, c = 0.535 nm for the solid solution of boundary composition, containing 50 mol % Gd_2O_3-50 mol % Fe_2O_3 (Table 1).

It should be noted that in the Fe_2O_3-La_2O_3 and Fe_2O_3-Nd_2O_3 systems at 1300 and 1400 °C, the perovskite phase has a clearly defined stoichiometric composition, not a region [24–25].

Journal of Chemistry and Technologies, 2025, *33*(4), 958-966

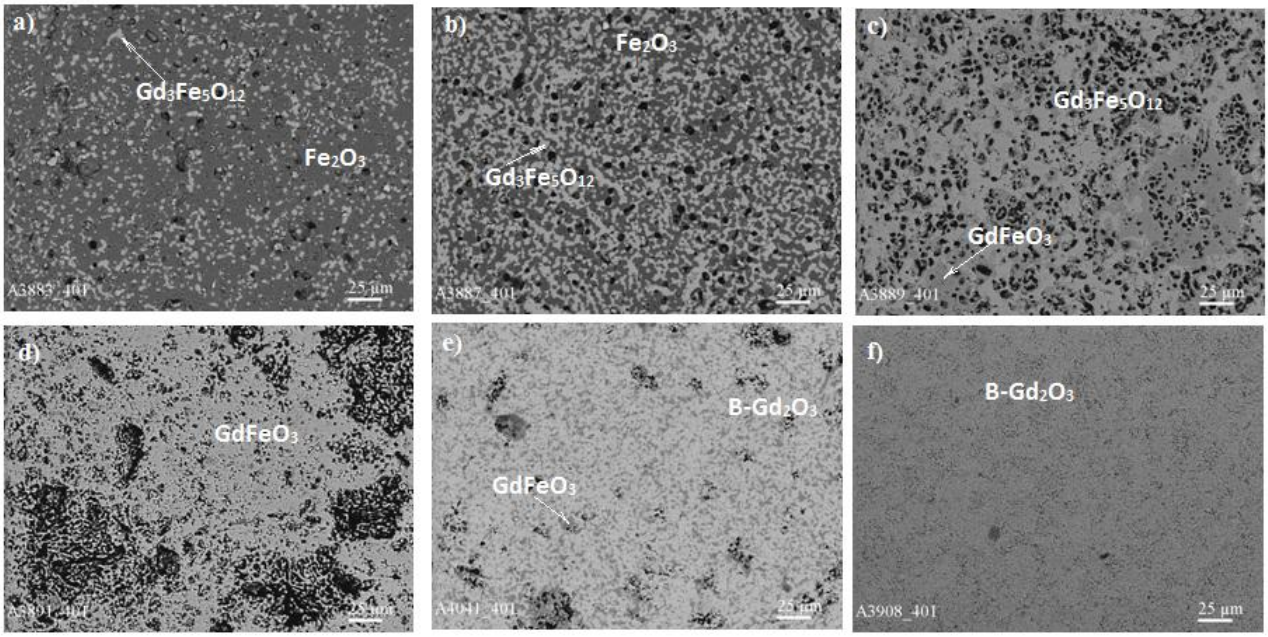

a **– 5 mol % Gd_2O_3-95 mol % Fe_2O_3;** ***b*** **– 15 mol % Gd_2O_3-85 mol % Fe_2O_3;** ***c*** **– 45 mol % Gd_2O_3-55 mol % Fe_2O_3;** ***d*** **– 49 mol % Gd_2O_3-51 mol % Fe_2O_3;** ***e*** **– 70 mol % Gd_2O_3-30 mol % Fe_2O_3;** ***f*** **– 98 mol % Gd_2O_3-2 mol % Fe_2O_3**

Fig. 2. SEM microstructures of the samples in the definite field of compositions of the system Fe_2O_3–Gd_2O_3 heat-treated at 1300 °C

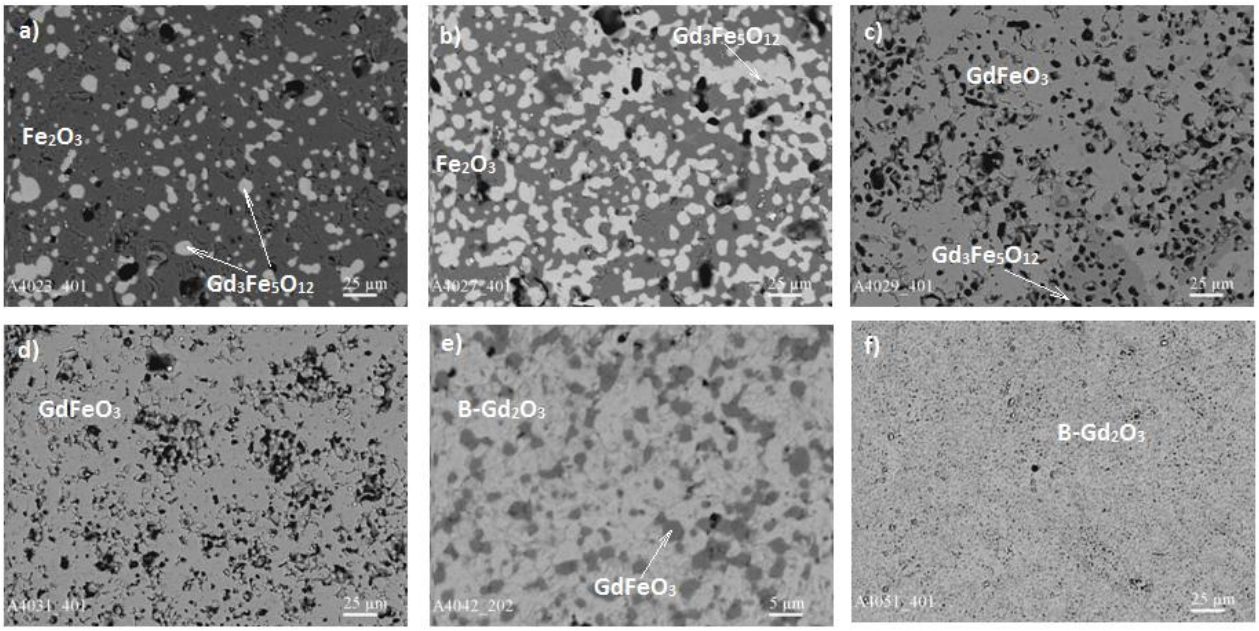

a **– 5 mol % Gd_2O_3-95 mol % Fe_2O_3;** ***b*** **– 15 mol % Gd_2O_3-85 mol % Fe_2O_3;** ***c*** **– 45 mol % Gd_2O_3-55 mol % Fe_2O_3;** ***d*** **– 49 mol % Gd_2O_3-51 mol % Fe_2O_3;** ***e*** **– 70 mol % Gd_2O_3-30 mol % Fe_2O_3;** ***f*** **– 98 mol % Gd_2O_3-2 mol % Fe_2O_3**

Fig. 3. SEM microstructures of the samples in the definite field of compositions of the system Fe_2O_3–Gd_2O_3 heat-treated at 1400 °C

Journal of Chemistry and Technologies, 2025, *33*(4), 958-966

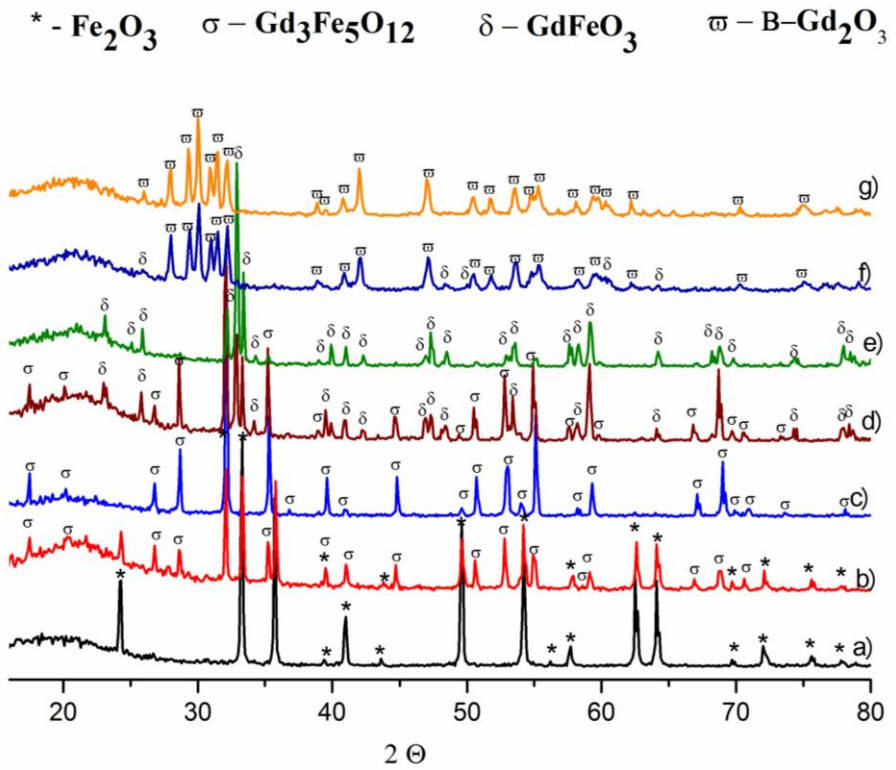

a **– 0 mol % Gd_2O_3-100 mol % Fe_2O_3;** ***b*** **– 5 mol % Gd_2O_3-95 mol % Fe_2O_3;** ***c*** **– 65 mol % Gd_2O_3-35 mol % Fe_2O_3;** ***d*** **– 45 mol % Gd_2O_3-55 mol % Fe_2O_3;** ***e*** **– 50 mol % Gd_2O_3-50 mol % Fe_2O_3;** ***f*** **– 95 mol % Gd_2O_3-5 mol % Fe_2O_3;** ***g*** **– 99 mol % Gd_2O_3-1 mol % Fe_2O_3**

Fig. 4. XRD of the samples in the definite field of compositions of the system Fe_2O_3–Gd_2O_3 heat-treated at 1300 °C

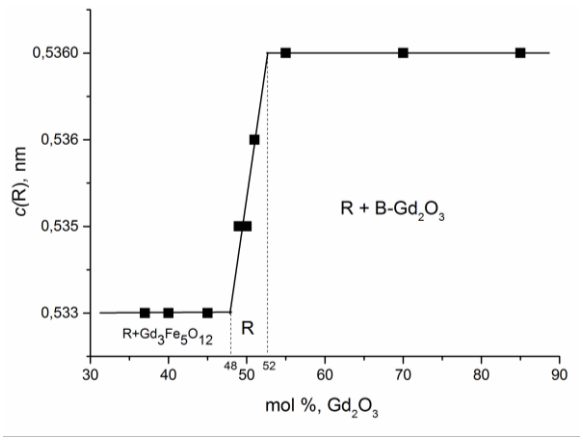

a)

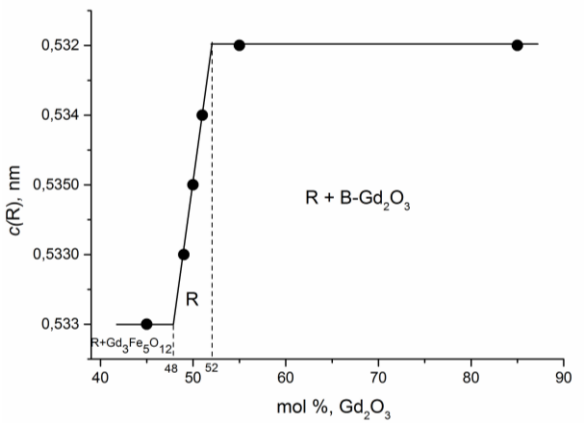

b)

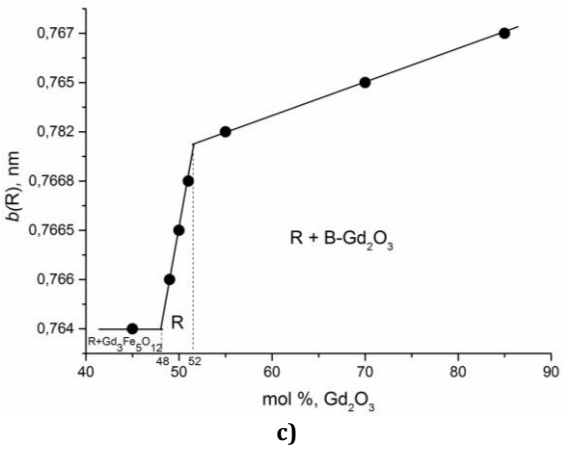

c)

Fig. 5. Concentration dependence of lattice parameters for solid solutions based on R in the system Fe_2O_3–Gd_2O_3 heat-treated at 1300 (a) and 1400 (b, c) °C

Journal of Chemistry and Technologies, 2025, *33*(4), 958-966

It was found that at 1300 °C and 1400 °C, the homogeneity region of the $Gd_3Fe_5O_{12}$ phase is in the range from 34 to 37 mol% Gd_2O_3, Fig. 6. The lattice parameters of the unit cell $Gd_3Fe_5O_{12}$ phase varies from a = 1.247 and 1.245 nm in two-phase samples ($Gd_3Fe_5O_{12}$ + Fe_2O_3 and $Gd_3Fe_5O_{12}$+ R), containing 30 mol % Gd_2O_3-60 mol % Fe_2O_3 and 37 mol % Gd_2O_3-63 mol % Fe_2O_3 to a = 1.246 nm in single-phase sample for composition, containing 35 mol % Gd_2O_3-65 mol % Fe_2O_3 (Table 1, Fig. 6).

In the Fe_2O_3-Nd_2O_3 system at 1300 and 1400 °C, the cubic phase of the $Ln_3Fe_5O_{12}$ type does not form [25].

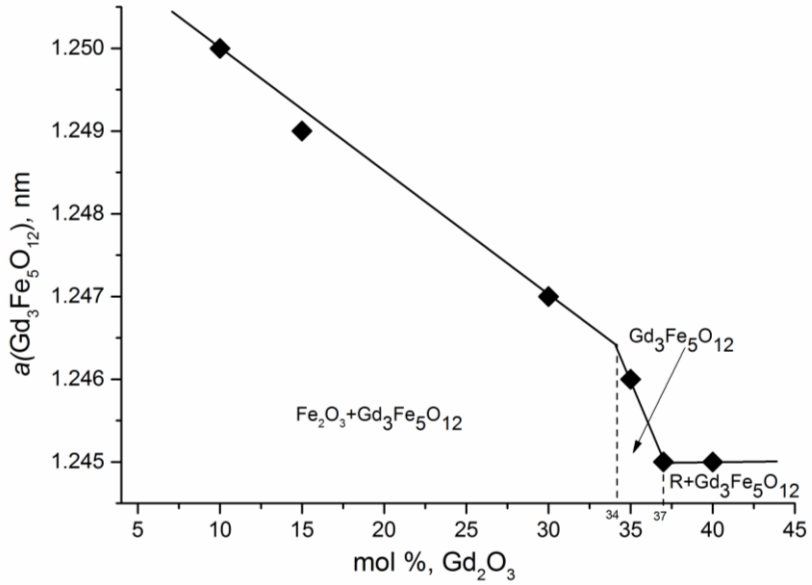

Fig. 6 Concentration dependence of lattice parameters for solid solutions based on $Gd_3Fe_5O_{12}$ in the system Fe_2O_3–Gd_2O_3 heat-treated at 1300 °C

Gd_2O_3 forms solid solutions based on the monoclinic modification. Using concentration dependencies of the parameters of the unit cell, it was shown that the homogeneity region of solid solutions based on the B phase extends from 97 to 100 mol% Gd_2O_3 at 1300 and 1400 °C, Table 1, Table 2, Fig. 7.

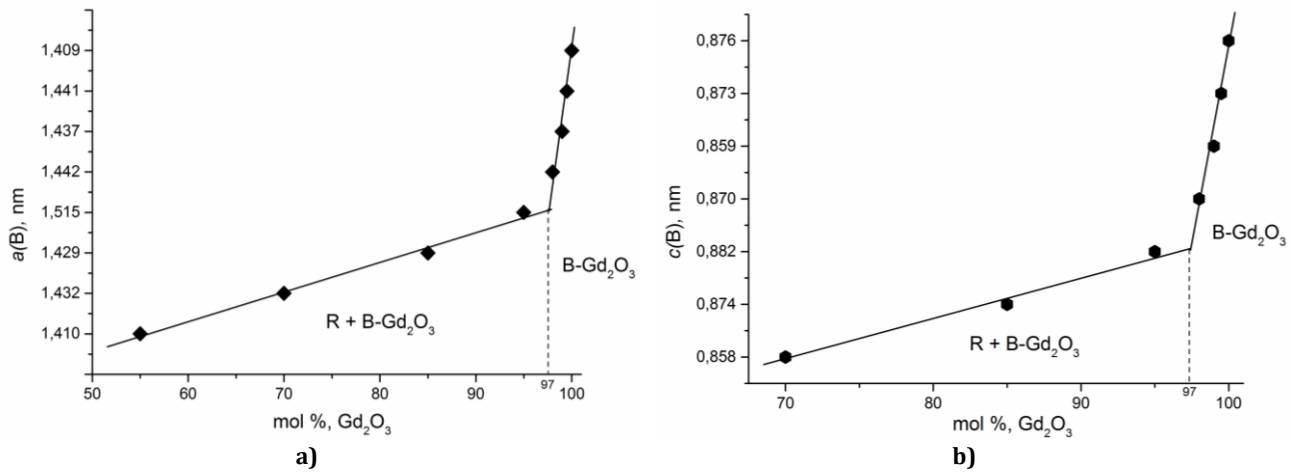

Fig. 7. Concentration dependence of lattice parameters for solid solutions based on B-Gd_2O_3 in the system Fe_2O_3–Gd_2O_3 heat-treated at 1300 (a) and 1400 (b) °C

The lattice parameters of the unit cell B-Gd_2O_3 phase varies from a = 1.515 nm, b = 0.358 nm, c = 0.958 nm, β = 92.15 in two-phase samples (B-Gd_2O_3 + R), containing 95 mol % Gd_2O_3-5 mol % Fe_2O_3 to a = 1.442 nm, b = 0.357 nm, c = 0.879 nm, β = 84.86 in single-phase sample for composition, containing 98 mol% Gd_2O_3-2 mol% Fe_2O_3 (Table 1).

The Fe_2O_3 does not form regions of homogeneity, Fig. 1, Table 1, Table 2.

Conclusions

Phase equilibria have been studied in the Fe_2O_3–Gd_2O_3 system at 1300 and 1400 °C. It has been established that solid state interactions between two oxides resulted in the formation of phases (B-Gd_2O_3, $GdFeO_3$, $Gd_3Fe_5O_{12}$, Fe_2O_3). The ordered phase $GdFeO_3$ (R) has a homogeneity region of 48–52 mol% Gd_2O_3 at both temperatures. The homogeneity region of the $Gd_3Fe_5O_{12}$ phase is 34–37 mol% Gd_2O_3 at 1300 °C and 1400 °C. For solid solutions based on the B phase, the homogeneity region extends from 97 to 100 mol% Gd_2O_3.

Acknowledge

This work supported by the research project of the NAS of Ukraine “New photocatalytic materials based on perovskite-type phase”

References

[1] Zhang, F., Huang, X., Qian, C., Zhu, L., Hida, N., Niu, G., Chen, X. (2012). Synergistic enhancement of iron oxide nanoparticle and gadolinium for dual-contrast MRI. Biochem. Biophys. Res. Commun., 425(4), 886–91. https://doi.org/10.1016/j.bbrc.2012.07.168

[2] Loai, Y., Ganesh, T., Cheng, H.L.M. (2012) Concurrent Dual Contrast for Cellular Magnetic Resonance Imaging Using Gadolinium Oxide and Iron Oxide Nanoparticles. *Int. J. Mol. Imaging*., 230942. https://doi.org/10.1155/2012/230942

[3] Zeng, Y., Wang, L., Zhou, Z., Wang, X., Zhang, Y., Wang, J., Mi, P., Liu, G., Zhou, L. (2017). Gadolinium hybrid iron oxide nanocomposites for dual T1- and T2-weighted MR imaging of cell labeling. *Biomater. Sci., 5*, 50–6. https://doi.org/10.1039/C6BM00706F

[4] Khumaeni, A., Avicenna, S., Nurhasanah, I. (2024). Synthesis of iron oxide-gadolinium oxide nanocomposite produced by pulse laser ablation in carboxy methylcellulose as a contrast agent of magnetic resonance imaging. *J. Mater. Sci. Mater. Electron., 35*, 1422. https://doi.org/10.1007/s10854-024-13198-9

[5] Montiel Schneider, M.G., Rivero, P.S., Muñoz Medina, G.A., Sanchez, F.H., Lassalle, V.L. (2023). $Gd(OH)_3$ as Modifier of Iron Oxide Nanoparticles—Insights on the Synthesis, *Characterization and Stability. Colloids Interfaces, 7*(1), 8. https://doi.org/10.3390/colloids7010008

[6] Pradhan, P.K., Panda, A.B., Mishra, G.K., Mohanty, N.K. (2025). Rare earth orthoferrites (RFeO3, R=rare earth elements): A comprehensive review of structural, dielectric, and magnetic properties. *Smart. Mater. Manuf., 3*, 100082. https://doi.org/10.1016/j.smmf.2025.100082

[7] Shen, H., Zhao, Y., Li, L., Li, Q., Geng, H., Li, Y., Shen, X., Xu, J., Zhou, D., Tian, T., Ma, Y., Shang, J., Wu, A. (2024). Recent advances of rare earth iron garnet magneto-optical single crystals. *J. Cryst Growth., 631*, 127626. https://doi.org/10.1016/j.jcrysgro.2024.127626

[8] Nakhaei, M., Bremholm, M., Khoshnoud, D.S. (2021). Structural and Magnetic Properties of RMO3 (R = Pr, Nd and M = Fe, Co) Perovskites. *J. Supercond. Nov. Magn., 34*, 3255–66. https://doi.org/10.1007/s10948-021-05992-x

[9] Li, C.L., Zheng, S.S., Barasa, G.O., Zhao, Y.F., Wang, L., Wang, C.L., Lu, Y., Qiu, Y., Cheng, J.B., Luo, Y.S. (2021). A comparative study on magnetic behaviors and magnetocaloric effect in heavy rare-earth antiferromagnetic orthoferrites RFeO3 (R=Dy, Ho and Er). *Ceram Int., 47*(24), 35160–9. https://doi.org/10.1016/j.ceramint.2021.09.059

[10] Chen, B., Katayama, T. (2023). Hexagonal $RFeO_3$ (R = Dy, Er, and Lu) Films Grown on Glass Substrates with Both Magnetic and Ferroelectric Orders. *ACS Appl Electron Mater., 5*(1), 344–9. https://doi.org/10.1021/acsaelm.2c01356

[11] Cho, E., Klyukin, K., Su, T., Kaczmarek, A., Ross, C.A. Composition-Dependent Ferroelectricity of $LuFeO_3$ Orthoferrite Thin Films. *Adv. Electron Mater., 9*(3), 2300059. https://doi.org/10.1002/aelm.202300059

[12] Pinho, S.L.C. (2018). Synthesis and Characterization of Rare-Earth Orthoferrite $LnFeO_3$ Nanoparticles for Bioimaging. *Eur. J. Inorg Chem., 468*. https://doi.org/10.1002/ejic.201800468

[13] Massa, N.E., Campo, L., Ta Phuoc, V., Alonso, J.A., Kayser, P. (2023). Low-temperature terahertz spectroscopy of $LaFeO_3$, $PrFeO_3$, $ErFeO_3$, and $LuFeO_3$: Quasimagnon resonances and ground-state multiplet transitions. *Phys. Rev. B., 108*, 115116. https://doi.org/10.1103/PhysRevB.108.115116

[14] Weber, M., Guennou, M., Zhao, H.J., Iñiguez-González, J., Vilarinho, R., Kreisel, J. (2016). Raman spectroscopy of rare-earth orthoferrites $RFeO_3$ (R=La, Sm, Eu, Gd, Tb, Dy). *Phys. Rev. B., 94*(21), 214103. https://doi.org/10.1103/PhysRevB.94.214103

[15] Naseri, M.G., Tran, H.L.T., Nguyen, U.T., Nguyen, T.L. (2020). Sol-gel synthesis and the investigation of the properties of nanocrystalline holmium orthoferrite. *Nanosyst. Phys. Chem. Math., 11*(6), 698–704. https://doi.org/10.17586/2220-8054-2020-11-6-698-704

[16] Chawda, N., Basu, M., Majumdar, D., Poddar, R., Mahapatra, S.K. (2019). Engineering of Gadolinium-Decorated Graphene Oxide Nanosheets for Multimodal Bioimaging and Drug Delivery. *ACS Omega., 4*(7),12470–9. https://doi.org/10.1021/acsomega.9b00883

[17] Usman, M.S., Hussein, M.Z., Fakurazi, S., Ahmad Saad, F.F. (2017). Gadolinium-based layered double hydroxide and graphene oxide nano-carriers for magnetic resonance imaging and drug delivery. *Chem. Cent. J., 11*, 47. https://doi.org/10.1186/s13065-017-0275-3

[18] Gwon, H., Kim, H., Lee, S. (2025). Gadolinium oxide-decorated graphene oxide-based dual-stimuli-responsive smart fluids. *Nanoscale, 17*, 5869–77. https://doi.org/10.1039/D4NR04941A

[19] Zhu, X.H., Xiao, X.B., Chen, X.R., Liu, B.G. (2017). Electronic structure, magnetism and optical properties of orthorhombic $GdFeO_3$ from first principles. *RSC Adv., 7*, 4054–61. https://doi.org/10.1039/C6RA25259A

[20] Musić, S., Ilakovac, V., Ristić, M. (1992). Formation of oxide phases in the system Fe_2O_3–Gd_2O_3. *J. Mater. Sci., 27*, 1011–5. https://doi.org/10.1007/BF01197655

[21] Musić, S., Popović, S., Czakó-Nagy, I., Gashi, F. (1993). Formation of oxide phases in the system Fe_2O_3–Gd_2O_3 Part II. *J. Mater. Sci. Lett., 11*, 869–73.

[22] Buscaglia, V., Buscaglia, M.T., Giordano, L., Martinelli, A., Viviani, M., Bottino, C. (2002). Growth of ternary oxides in the Gd_2O_3–Fe_2O_3 system. A diffusion couple study. *Solid State Ionics., 146*(3–4), 257–71. https://doi.org/10.1016/S0167-2738(01)01021-9

[23] Khan, M.S., Mukherje, A., Kumaresan, R. (2025). Electrochemical deoxidation behavior of Gd_2O_3 Fe_2O_3 oxides in LiCl and $CaCl_2$ melts. *J. Appl. Electrochem., 55*, 1601–14. https://doi.org/10.1007/s10800-024-02256-z

[24] Chudinovych, O. V., Vedel, D.V., Stasyuk, O.O., Tomila, T.V., Aguirre, M.H. (2024). Production, structure and magnetic properties of nanocomposites based on the perovskite phase $LaFeO_3$. *Solid State Sci., 157*, 107699. https://doi.org/10.1016/j.solidstatesciences.2024.107699

[25] Chudinovych, O. V., Vedel, D.V., Stasyuk, O.O., Samelyuk, A. V., Aguirre, M.H. (2024). Phase relations in the Nd_2O_3-Fe_2O_3 system: Structure andmagnetic properties of perovskite NdFeO3 ceramics. *Process. Appl. Ceram., 18*(3), 314–322. https://doi.org/10.2298/PAC2403314C